Using 7T susceptibility-weighted imaging to aid in the characterization of high-grade gliomas

J. M. Lupo[1], S. M. Chang[2], and S. J. Nelson[1,3]

[1]Department of Radiology, University of California, San Francisco, California, United States, [2]Department of Neurological Surgery, University of California, San Francisco, California, United States, [3]Program in Bioengineering, University of California, San Francisco, California, United States

Introduction

Susceptibility-weighted imaging (SWI) is a powerful tool for high resolution imaging of the vasculature [1] that has been shown to improve the diagnosis of brain neoplasms at low field strengths [2]. At 7 Tesla, the enhanced sensitivity to microvasculature due to higher susceptibility effects can provide a major advantage by allowing the detection of vessels or microhemorrhages as small as 100-200μ. Application of a GRAPPA-based acquisition at 7T has facilitated the use of SWI in patient studies, revealing regions of microhemorrhages in normal brain tissue due to radiation, the recruitment of large blood vessels in active tumor regions, and the accumulation of blood products and/or calcification [3]. Previous work has shown high correlation between the hypointensity on 3T SWI images with rCBV in normal brain tissue, but no trend was observed within the tumor [4]. The goal of this study is to further investigate the unique contrast present in SWI images of high-grade glial tumors by analyzing the overlap of 7T SWI hypointensity with the T2 hyperintensity region, contrast-enhancing lesion, and perfusion abnormality at 3T.

Methods

Acquisition: Sixteen high-grade glioma patients (10 grade III and 6 grade IV), all of whom had received prior treatment, were scanned on a 3T GE Signa Echospeed system with 8-channel phased array receive coil (Medical Devices) and body coil excitation and 7T whole body GE scanner, using uniform excitation by a volume transmitter and reception by an 8-channel head coil (Nova Medical). High resolution T2*-weighted SWI was acquired at 7T using a 3D flow compensated SPGR sequence with TE/TR 16/80ms, flip 20°, 24cm FOV, and employed either an image matrix of 512x256, 512x144 with GRAPPA R=2, or 512x102x28 with GRAPPA R=3. The GRAPPA acquisitions included 16 AC lines and were reconstructed with a GRAPPA-based technique developed by our group [3]. The coverage in z was varied to image the extent of the entire tumor at 1mm resolution. A 2D T2*-weighted GRE (TE/TR 11.4/30ms, flip 20°, 18cm FOV, 512x512 matrix, 10 slices, 2mm/4mm slice thk/gap) was also acquired and utilized as an intermediate for registration between 3T and 7T. The 3T imaging protocol included standard clinical pre- and post-contrast T1-weighted SPGR images, T2-weighted FLAIR images, and either T2*-weighted (TE/TR=54/1500ms, flip 35°, 26cm FOV, 128×128 matrix, 4mm slice thk, 80 time pts) or T1-weighted (TE/TR=1.14/4.5, flip 20°, 26cm FOV, 256x256 matrix, 3mm slice thk) dynamic perfusion imaging.

Post-processing: The 3T T2 FLAIR, post-contrast T1 SPGR, and perfusion volumes were registered to the 7T SWI images through rigid body transformations that maximized the normalized mutual information [5], utilizing the pre-contrast T1-weighted SPGR image as an intermediate reference to co-register the images. The SWI processing employed a 96x96 Hanning filter and the resulting phase mask was multiplied with the magnitude image four times. A low pass filter with edge completion was applied to the combined images and minimum intensity projections (mIPs) through 4 mm thick slabs were generated to obtain the final SWI images used for analysis. The aligned 3T images were then resampled and restricted to the FOV of the SWI mIP images. Regions of contrast-enhancing tumor (CEL), T2-hyperintensity (T2h), and resection cavity were manually defined from the registered T2 FLAIR and post-contrast T1 SPGR images.

Results & Discussion

Volumes: The T2h volume was at least twice as large as the volume of SWI abnormality in all but three patients. No trend was observed between the size of the CEL and SWI lesions. Volumes of SWI and T2h lesions were similar between grades while the median CEL volume was twice as large in grade IV patients.

Overlap of 3T clinical images with 7T SWI: The T2h region had a larger region that overlapped with SWI compared to the portion of the CEL that coincided with SWI hypointensity. However, a 3.4-fold increased in percent overlap of the CEL with SWI was observed in grade IV gliomas compared to grade III patients. This is evident in Figs. 1 & 2 where the SWI hypointensity in the two representative grade III gliomas (Fig. 2 & Fig. 3, *top*) does not overlap with the CEL (in red), whereas the grade IV glioma (Fig. 2, *bottom*) shows overlap between the two.

Overlap of SWI and perfusion abnormality: In 8/15 patients SWI hypointensity coincided with regions of elevated blood volume, while 12/15 patients exhibited microvascular leakage where SWI hypointensity was present. Fig. 1 demonstrates an example where the SWI hypointensity concurs with elevated vessel volume rather than leakage while the example shown in Fig. 2 (*top*) illustrates the opposite effect. In Fig. 2 (*bottom*), the SWI hypointensity overlaps with both abnormal perfusion regions.

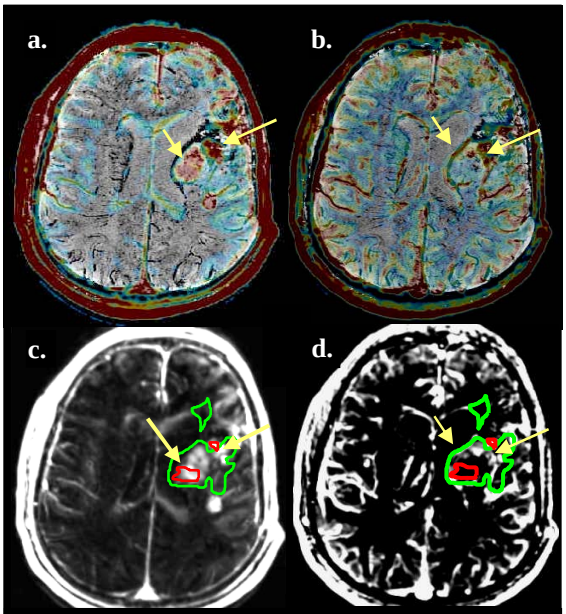

Fig. 1: a) leakage & b) blood volume maps, overlaid on 7T SWI. In c) and d), maps from a) and b) with CEL & T2h regions.

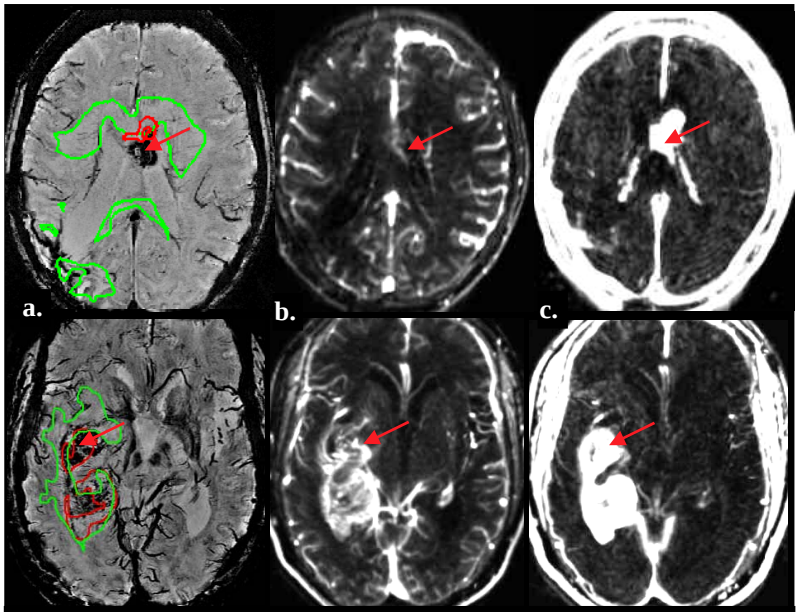

Fig. 2: a) 7T SWI images with CEL & T2h regions with corresponding b) blood volume maps & c) leakage maps for representative grade III (top) and grade IV (bottom) glioma

Conclusions

SWI provides unique and potentially valuable contrast that is not always present on conventional anatomical or perfusion scans, highlighting heterogeneity within the contrast enhancing lesion and regions of elevated blood volume or blood-brain-barrier compromise. Future studies are necessary to explore the biological basis behind the hypointensity observed on SWI images within the contrast-enhancing lesion that is not the result of abnormal vasculature and maybe due to microhemorrhages or calcification. This additional information is expected to be advantageous in assessing treatment effect and response for both anti-angiogenic and radio-therapy.

References: [1] Haacke EM *et al.* MRM 2004 52:612-8. [2] Sehgal V *et al.* JMRI 2005 22:439-45. [3] Lupo JM *et al.* Proc. 15th ISMRM 2007. [4] Lupo JM *et al.* Proc. 14th ISMRM 2006. [5] Jenkinson. MRM 2002 49:193-197. The research was supported by grants ITL-BIO04-10148, R01 CA059880, and P50 CA97257, and a Joelle Syverson American Brain Tumor Association Fellowship.